

Article

Tribological and Thermal Transport of Ag-Vegetable Nanofluids Prepared by Laser Ablation

Jaime Taha-Tijerina ^{1,*}, Sadasivan Shaji ², Sreed Sharma Kanakillam ²,
Maria Isabel Mendivil Palma ³ and Karla Aviña ¹

¹ Engineering Department, Universidad de Monterrey, Av. Morones Prieto 4500 Pte., San Pedro Garza García 66238, N. L., Mexico; karla.avina@udem.edu

² Facultad de Ingeniería Mecánica y Eléctrica, Universidad Autónoma de Nuevo León, Av. Universidad S/N San Nicolás de los Garza, Nuevo León 66450, Mexico; sadasivan.shaji@uanl.edu.mx (S.S.); sreedsharma@gmail.com (S.S.K.)

³ Centro de Investigación en Materiales Avanzados (CIMAV), Unidad Monterrey, Av. Alianza Norte 202. Parque PIIT, Apodaca, Nuevo León 66600, Mexico; maria.mendivil@cimav.edu.mx

* Correspondence: jose.taha@udem.edu

Received: 20 February 2020; Accepted: 28 February 2020; Published: 5 March 2020



Abstract: Lubricants and fluids are critical for metal-mechanic manufacturing operations as they reduce the friction and wear of tooling and components, and serve as coolants to dissipate the heat generated in these operations. The proper application of these materials improves machine operative life and tooling, and decreases cost, energy, and time consumption for maintenance, damage, repairs, or the need to exchange pieces/components within the machinery. Natural or vegetable-based lubricants have emerged as a substitute for mineral oils, which harm the environment due to their low biodegradability and have negative effects on human health (e.g., causing skin/respiratory diseases). Thus, finding biocompatible and efficient lubricants has become a technology objective for researchers and industry. This study evaluates soybean-, corn-, and sunflower-based lubricants reinforced with silver (Ag) nanostructures by a pulsed laser ablation process. Thermal and tribological evaluations were performed with varying Ag contents, and temperature-dependent behavior was observed. Thermal conductivity improvements were observed for all nanofluids as the temperature and Ag concentration increased (between 15% and 24%). A maximum improvement of 24% at 50 °C and 10 min exposure time of the pulsed laser ablation process for soybean oil was observed. The tribological evaluations showed improvements in the load-carrying capacity of the vegetable oils, i.e., an increase from 6% to 24% compared to conventional materials. The coefficient of friction performance also showed enhancements with Ag concentrations between 4% and 15%.

Keywords: tribology; lubricant; thermal conductivity; silver; laser ablation

1. Introduction

In metal-mechanic processes, using the appropriate type of fluids and lubricants, together with the proper working materials, could reduce the friction and wear of machinery and tooling components. This also increases machine efficiency in terms of workpiece surface finish and tolerances, thus improving machines' operative life and eventually reducing the vibrations and required cutting force [1–5]. According to Oakridge National Laboratory (USA), wear and friction contribute to about 25% of worldwide total energy loss [6].

Approximately 85% of lubricants used worldwide are petroleum based [7]. The ecological issues related to the extensive usage of these oils and the geopolitical strategies regarding crude oil exploitation are the main drivers for the development of novel alternatives from eco-friendly raw materials [8–10].

To prevent adverse effects on industrial operators and the environment, intensive research concerning improved cooling and lubrication performance is recommended.

Fluids and lubricants have an impact on heat dissipation and metal-mechanic process parameters such as cutting speed, feed rate, and depth of cut [11]; they also provide a proper working component interface, i.e., help in washing away chips and debris from machined surfaces. Natural lubricants, such as soybean, sunflower, and corn oils, act as antifriction components, which facilitate these manufacturing processes while reducing the risks associated with machinery damage or failures.

According to Celik et al. [10], “green” processing should be one of the most common methods applied to obtain the optimum output of machine components. During machining, the coolant and lubricant performance must be favorable to improve quality and productivity. Elevated temperatures, high pressures, and other processing factors cause a more rapid deterioration of fluids and lubricants, leading to problems caused by their frequent replacement, and thus, increasing industrial production costs. Furthermore, the usage of these materials has various disadvantages, such as environmental impact, increased material costs, and health hazards, i.e., respiratory and skin diseases due to their toxic or nonbiodegradable characteristics [10,12–16].

Recently, vegetable fluids are getting more attention as novel potential alternatives to petroleum-based lubricants or coolants due to their inherent properties and performance, such as being renewable, biodegradable, and nontoxic. It has been observed that vegetable fluids minimize carbon monoxide emission levels, which is one of the main reasons for their increased application in the industrial field. Vegetable fluids possess excellent biodegradability with excellent applicability to tribological problems. Although natural or vegetable fluids have excellent properties and applicability, they also have certain drawbacks that affect their performance. However, vegetable fluids have shown limited industrial applicability due to their low temperature performance [17–19], poor thermal or oxidation stability [19–25], and the occurrence of other tribochemical degrading processes [26–28] under specific working conditions of pressure, stress, temperature, and environment. A critical problem with vegetable fluids is their limited oxidative stability, which adversely impacts their shelf life and performance [29–31]. For instance, a low oxidative stability results in a faster oxidizing rate; consequently, the fluid polymerizes and becomes thick [32]. The oxidative instability of vegetable lubricants is attributed to the structural “double bond” in the fatty acid part of the β -CH group of the alcoholic (glycerin) components [31]. Furthermore, vegetable fluids chemically interact with metallic working surfaces at high temperatures, forming a high strength fluid film or layer, resulting in reduced friction and wear. These strong intermolecular interactions are resistant to temperature alterations, which results in high viscosity [33].

Pulsed laser ablation in liquid (PLAL) is a “green” method to synthesize nanostructures starting from bulk targets by laser irradiation. While the main mechanism of nanostructure or nanoparticle production is quite complex, the physical procedure is a simple matter of exposing a bulk target immersed in a solvent to a pulsed laser [34]. The ablation characteristics, such as pulse width and irradiation time, laser wavelength, ablation fluence (energy per unit area), as well as solvent characteristics, such as viscosity, dipole moment, and refractive index, determine the morphology and characteristics of the produced nanostructures [35,36]. The prime advantage of this technique is the procurement of surfactant free, well-dispersed nanostructures in the surrounding liquid without any toxic chemical reactants or waste [37]. The energy from the pulsed laser source is concentrated onto the target surface immersed in the liquid medium. Photon absorption, heating, and thermal evaporation are the main mechanisms for nanosecond-pulsed lasers in the process. As is well known, a plasma is generated where the laser energy is focused, which contains evaporated atoms, molecules, and radicals from the target. This plasma is contained by the surrounding fluid medium which causes the formation of a cavitation bubble. The extremely high temperature and pressure of the cavitation bubble cause its expansion and then collapse, regularly triggering the release of nanostructures into the surrounding medium [34]. In addition to the laser characteristics, such as wavelength, pulse energy, pulse duration, and repetition rate, the diverse characteristics of the liquid medium, such as, viscosity,

heat capacity, refractive index, dielectric constant, among others, are also important in determining the size and morphology of the produced nanostructures.

PLAL was successfully applied to obtain surfactant-free, stable nanofluids of metals, magnetic materials, semiconductors, and ceramics. Based on our previous research, we can successfully synthesize nanofluids of metals, metal oxides, ceramics, and semiconductors. Furthermore, thin films, which were deposited from their respective nanofluid suspensions using spin-coating and dip-coating methods, were produced from these semiconductor nanofluids [38–41].

As for sunflower, soybean, and corn oils, past studies have described how heat is dissipated and how their tribological performance can be improved. Therefore, this experimental study shows the effects on Ag-nanostructures by a pulsed laser ablation technique dispersed within vegetable lubricants to improve their tribological and heat-transfer characteristics, i.e., wear resistance, coefficient of friction (COF), load-carrying capacity, and thermal conductivity.

2. Materials and Methods

In the present study, three vegetable oils, i.e., sunflower (Sigma Aldrich, Toluca, México - CAS number: 8001-21-6), soybean (Sigma Aldrich, Toluca, México - CAS number: 8001-22-7), and corn (Sigma Aldrich, Toluca, México - CAS number: 8001-30-7) were used to obtain nanofluids reinforced with silver (Ag) (Table 1). Nanostructures of Ag were prepared within soybean, corn, and sunflower oil by the PLAL technique. A metallic target (50 mm in diameter and 6.35 mm in thickness) of high purity silver (99.99%) was purchased from Beijing Metals, China. For this synthesis process, a pulsed Nd:YAG laser source with a wavelength, frequency, and pulse duration of 532 nm, 10 Hz, and 10 ns, respectively, was applied.

Table 1. Material Properties.

Materials	Properties				
Vegetable Fluids	Density @ 20 °C (g/cm ³)	Viscosity @ 24 °C (m Pa s)	Viscosity @ 40 °C (m Pa s)	Viscosity @ 100 °C (m Pa s)	Refractive Index
Soybean Oil	0.9604	54.3	32.93	6.79	1.47
Corn Oil	0.9100	52.3	30.8	6.57	1.40
Sunflower Oil	0.9197	68.0	40.05	8.65	1.70

2.1. Nanofluids Preparation

To prepare the Ag-nanofluids, 55 mL of vegetable oil was taken in a glass beaker and the Ag target was immersed in it. A convex lens with a 50 cm focal length was used to concentrate the laser energy on the target. The immersed target within the lubricant was kept 30 cm from the lens. Laser pulse energy/area gives the fluence. An energy meter was used to measure the laser energy (300 mJ/pulse). The normal laser spot size was 10 cm. A lens with a 50 cm focal length was used in this study. The target was set at 30 cm apart from the lens. The actual laser spot size on the Ag target was 4 mm in diameter. The laser energy per area (fluence) was calculated as 2.4 J/cm². This laser fluence was used to prepare the nanostructures in various vegetable oils. After aligning the laser using the operation mode, and Q switch mode to obtain 10 nanosecond pulses with high energy, the pulsed laser enhanced mode was used for the ablation process using nanosecond pulses. The laser ablation was performed for 5 and 10 min to obtain two different concentrations of nanofluids. After every minute, a new spot on the target was ablated to avoid the effects of continuous irradiation at the same spot. Stable Ag-nanofluids were obtained in the lubricants. Ag-nanostructures were synthesized in isopropyl alcohol (IPA) for the same ablation time. The Ag nanostructures were evaluated for their morphology by scanning electron microscopy (SEM), average size by dynamic light scattering (DLS), concentration by an inductively coupled plasma–optical emission spectroscopy (ICP-OES), and elemental composition and chemical states by X-ray photoelectron spectroscopy (XPS).

2.2. Morphology by SEM

A morphological analysis of the silver nanostructures was performed by a Hitachi SU8020-scanning electron microscope. Samples were prepared by drying a few drops of the nanofluid on silicon substrates and analyzed in secondary electron mode for an applied acceleration voltage of 1 kV. Figure 1a,b depicts the Ag-nanostructures at two different magnifications, i.e., 20,000 \times and 40,000 \times ; in general, this process yields a spherical nanostructure morphology. Additionally, it was observed that some of the nanostructures aggregated to form chain-like nanostructures in the nanofluids. These were formed as an effect of pulsed laser ablation in the fluid in the absence of additives or surfactants.

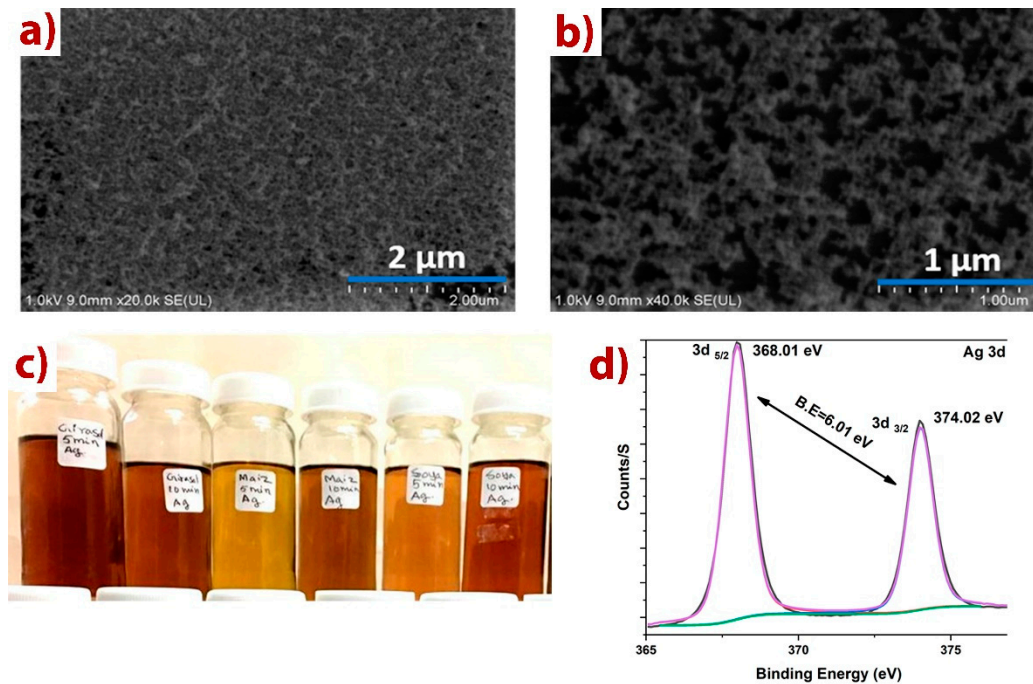


Figure 1. Ag nanostructure morphology by SEM at two different magnifications (a) 20,000 \times and (b) 40,000 \times . (c) Vials with different Ag-based nanofluids at various laser ablation times (5 and 10 min) and (d) X-ray photoelectron spectrum of the Ag-nanostructures.

The composition and chemical states of the nanostructures obtained by laser ablation was analyzed by the XPS technique. Thermo Scientific K-Alpha equipment for the XPS analysis was used. Figure 1d shows the high-resolution X-ray photoelectron spectrum of the Ag-nanostructures. The figure shows spin orbit split for Ag 3d photoelectron spectrum. The major intensity peak of Ag3d_{5/2} and lower intensity peak of Ag3d_{3/2} were at peak binding energies of 368.01 and 374.02 eV, respectively. These binding energy values agree with those of metallic silver [42]. The separation of the peaks was evaluated at 6.01 eV, which was also in agreement with the results reported in the literature [43,44]. A high-resolution spectral analysis confirmed that the nanostructures were in their elemental state.

2.3. Thermal Conductivity Characterization

The thermal conductivity of vegetable nanofluids at various concentrations and temperatures was measured by a transient hot-wire technique. The KD2 Pro equipment was calibrated using glycerol, and thermal conductivity results were verified to three decimal points. A thermal water bath was used for temperature-dependent evaluations. The specimens (40 mL glass vials) were thermally equilibrated for 10 min before each set of measurements. Thermal conductivities were compared with each of the control fluids at different temperatures. At least eight readings were measured for each set of experiments; the average values with standard deviation as error bars were reported and are discussed in this research.

2.4. Tribological Experimentation

Tribological characterization was evaluated with a four-ball tribotester configuration to obtain the load-carrying capacity under extreme pressures. In this tribotest, the nanofluids were subjected to a linearly increasing load from 0 to 7200 N, with a rotational speed of 500 rpms for 18 s (Table 2), where 12.7 mm diameter spheres of AISI 52,100 steel with 60 HRC were used [45]. The Institute for Sustainable Technologies - National Research Institute (ITEePib) Polish technique was selected due to the sensitivity to extreme pressure lubricants [1,46–49], as well as being less time consuming. In this study, when the frictional torque reached 10 N m, nanofluid seizure occurred and the nanofluid-“protective” film was destroyed; the load at this point corresponded to the seizure load (P_{oz}). If seizure did not occur by the end of the measurement, P_{oz} was 7200 N. The limiting pressure of seizure or p_{oz} , was calculated using Equation (1) as follows [45]:

$$p_{oz} = 0.52 \frac{P_{oz}}{WSD^2} \quad (1)$$

where p_{oz} is limiting pressure of seizure, P_{oz} is seizure load, and WSD is wear scar diameter.

Table 2. Four-ball tribotest evaluation parameters.

Parameters	ITEePib Polish Method
Time	18 s
Temperature (°C)	24 ± 1
Velocity (RPM)	500
Applied Force (N)	0–7200 (linear increment)

An Alicona IF-EdgeMaster optical 3D surface microscope was used to measure the average wear scar diameter of the three lower spheres, obtaining the average in millimeter to calculate the load-carrying capacity (p_{oz}) of the nanofluid; the greater the p_{oz} , the better the tribological characteristics of the lubricant.

3. Results

3.1. ICP-OES/Elemental Composition Analysis

The elemental composition was quantified using an ICP-OES (Thermo Scientific iCAP 6500—ICP-OES CID). It was observed that as the ablation time doubled, the concentration had no significant increase in nanostructure filler fraction; this might be due to the post irradiation effect of the nanofluids [50]. Thus, the particle size will be reduced further as the laser ablation time increases. It was observed that the concentrations of the nanostructures for 5 and 10 min pulsed laser irradiation in IPA were 5.54 mg/L and 6.55 mg/L, respectively.

3.2. DLS Analysis/Average Size Determination by DLS

The average size of silver nanostructures was determined by the DLS method by Zetasizer Nano ZS. The DLS readings of the obtained nanofluids by laser ablation for 5 min were as follows: sunflower oil 122 nm, corn oil 255 nm, soybean oil 172 nm, and IPA 67 nm. The DLS curves corresponding to the given values along with the polydispersity index (PDI) are shown in Figure 2. It can be observed that the size of nanostructures in IPA appeared to be smaller, whereas those in vegetable oils are bigger. This may be due to the density of the oil. In comparison to the vegetable oils, IPA has low density. Thus, during the nanostructure production by laser ablation, a plasma plume is formed in which the corresponding ions of the elements/compounds are present [36]. As the ablation process proceeds, the plasma plume expands and the nanostructures are liberated into the corresponding liquid medium. As the density varies, the time taken for plasma plume expansion also increases, which results in the production of larger particles or the agglomeration of smaller particles. These results will be influenced

by the temperature too, i.e., mainly by the boiling point of the vegetable oils. The refractive indexes of the vegetable oils used for DLS measurements are tabulated in Table 1.

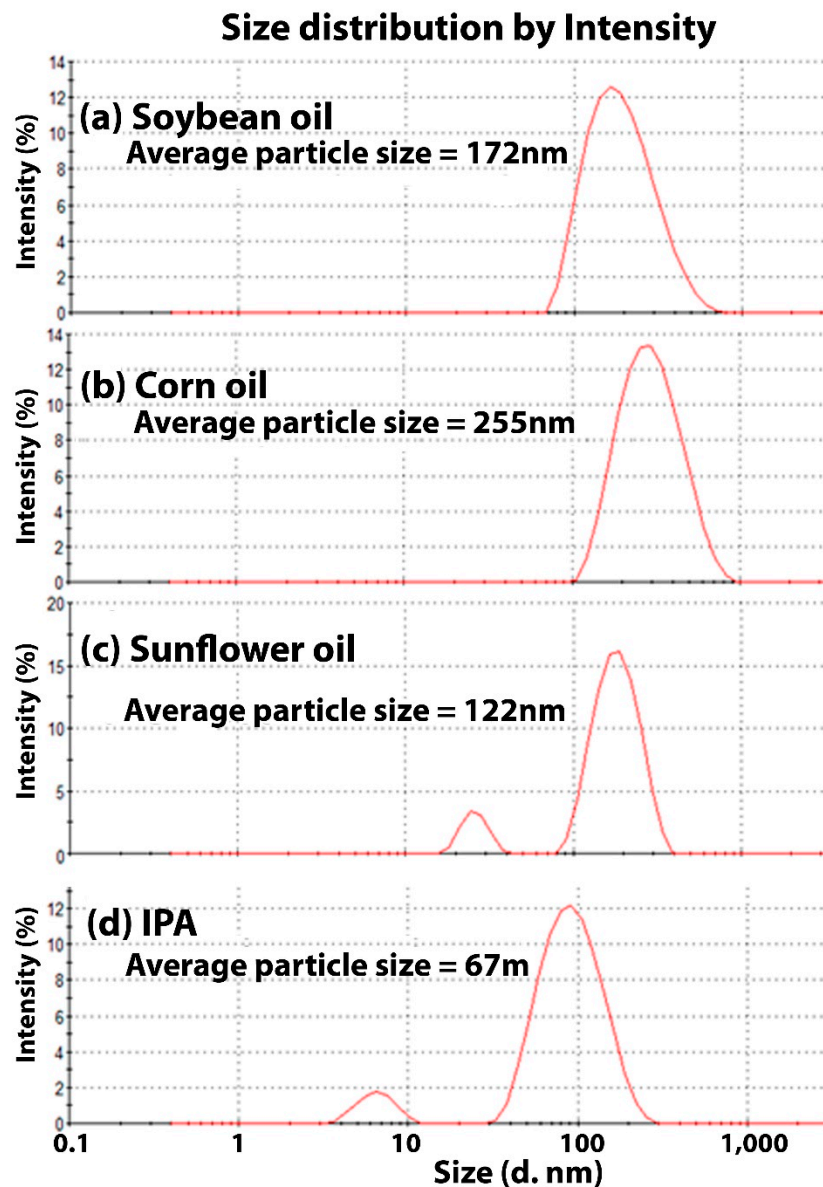


Figure 2. DLS curves of Ag-nanostructures in (a) Soybean oil ($PDI = 0.142$), (b) Corn oil ($PDI = 0.215$), (c) Sunflower oil ($PDI = 0.334$) and (d) IPA ($PDI = 0.492$).

4. Results and Discussion

4.1. Thermal Performance

Figure 3 shows the thermal conductivity performance in the temperature-dependent evaluations for the investigated vegetable nanofluids. It was observed that conventional vegetable oils were not significantly affected by the temperature dependence evaluation (i.e., less than 2% increase at 50 °C, compared to room temperature).

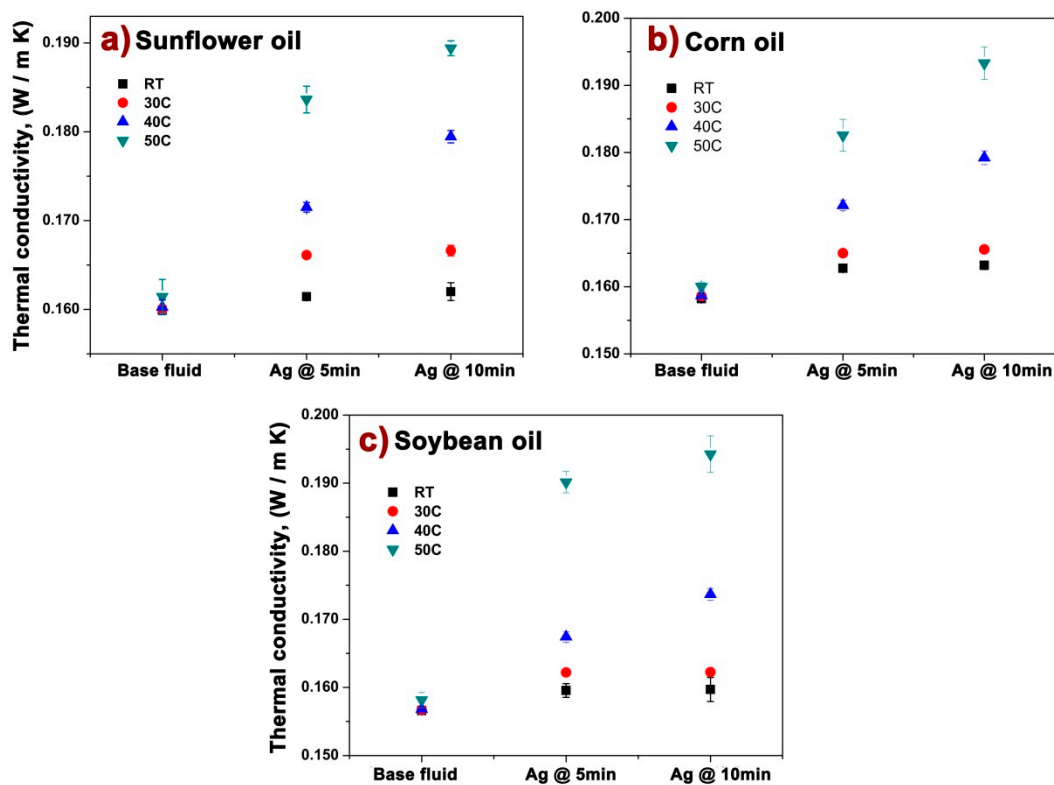


Figure 3. Thermal conductivity enhancement of vegetable nanofluids at 5 and 10 min laser ablation times. (a) Sunflower oil, (b) Corn oil and (c) soybean oil.

For sunflower oil, improvements of 15% and 18% were observed at 50 °C for 5 and 10 min of laser ablation, respectively. Similarly, soybean oil showed an improvement of 21% and 24% at 5 and 10 min of laser ablation, respectively. The effects on corn oil were also satisfactory, showing a 15% and 21% increase at 5 and 10 min of laser ablation, respectively (Figure 3).

The thermal conductivity of nanofluids increases with increasing temperature and laser ablation process time. This indicates the influence of Ag nanostructures on thermal conductivity [51–53], and demonstrates the influence of Brownian motion in the thermal transport behavior [54,55].

4.2. Tribological Performance

Figure 4 shows a comparison of the p_{oz} of various vegetable nanosystems. Sunflower oil showed an increase in the load-carrying capacity of 14% and 24% with 5 and 10 min of laser ablation, respectively. Similarly, soybean oil exhibited an improvement of 16% and 23% with 5 and 10 min of laser ablation, respectively. The Ag-laser ablation process on corn oil also showed improvement in load-carrying capacity by 6% and 10% with 5 and 10 min of laser ablation, respectively.

Diverse studies have presented the roles of nanomaterials in fluids and lubricants [56,57] in which similar behavior is observed. The frictional power losses are reduced due to the nanostructure mechanism that converts the sliding to rolling friction and the formation of tribofilms on the contact surfaces. The tribological improvement of Ag nanostructures could be due to a tribosintering effect on the surfaces, and the spacer effect could be due to their small size and interlayer interactions within vegetable oils.

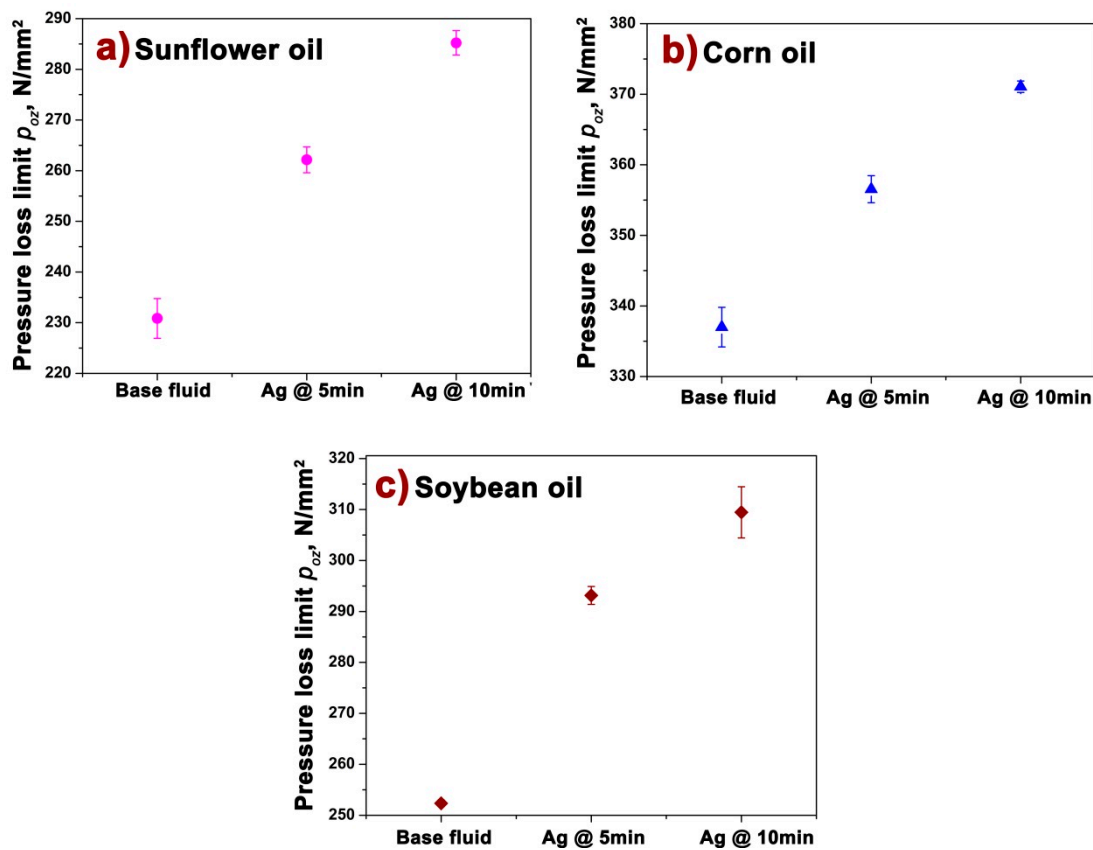


Figure 4. Tribological performance of Ag-vegetable nanofluids at 5 and 10 min laser ablation times. (a) Sunflower oil, (b) Corn oil and (c) soybean oil.

The effects on COF during tribotesting under scuffing conditions by Ag nanostructures dispersed by pulsed laser ablation within vegetable oils are shown in Table 3.

Table 3. COF performance at 5 and 10 min of Ag nanostructures by laser ablation.

	Pure	Ag	
		5 min	10 min
<i>COF-μ</i>			
Soybean Oil	0.0385 ± 0.0009	0.0365 ± 0.0004	0.0345 ± 0.0004
Corn Oil	0.0485 ± 0.0006	0.0467 ± 0.0004	0.0445 ± 0.0003
Sunflower Oil	0.0437 ± 0.0005	0.0402 ± 0.0003	0.0372 ± 0.0003

5. Conclusions

In the present study, a tribological and thermal transport evaluation of environmentally friendly, pulsed laser ablated, Ag-based vegetable nanofluids was performed. Soybean, sunflower, and corn oils were used as liquid media to trigger bulk silver by laser irradiation. The incorporation of silver nanostructures within these natural lubricants showed overall positive results.

It was observed that the irradiation time had significant effects on the nanofluids, and showed improvements in their tribological and heat-transfer characteristics. For instance, the limiting pressure of seizure improved compared to conventional lubricant, ranging from a 6% to 14% increase at 5 min irradiation, and up to a 24% increase at 10 min irradiation. This was attributed to the nanostructures displaying a rolling friction behavior, forming tribo-films, and tribosintering on the contact surfaces.

On the other hand, in general, all nanofluids showed a temperature-dependent behavior in thermal transport evaluations, also showing an interlayer interaction of silver with natural oils. Thermal conductivity improved in the range of 15% for 5 min ablation and up to 24% at 10 min ablation.

The results showed the potential of this laser ablation technique and the application of natural oils as coolants or for metal-forming processes. Increased environmental awareness is the main driving force for the development novel technologies. Therefore, biodegradable fluids for use in environmentally sensitive areas have great potential to succeed in industrial applications.

Author Contributions: Conceptualization, J.T.-T.; Methodology, J.T.-T., K.A., and S.S.; Validation, J.T.-T., S.S., and S.S.K.; Formal analysis, J.T.-T.; Investigation, J.T.-T., S.S., and S.S.K.; Resources J.T.-T. and S.S.; Data curation, K.A., S.S.K., and M.I.M.P.; Project administration, J.T.-T.; Supervision, J.T.-T., S.S.; Writing-original draft, J.T.-T.; Writing-review & editing, J.T.-T., S.S., K.A., and S.S.K. All authors have read and agreed to the published version of the manuscript.

Funding: This research received no external funding.

Acknowledgments: Authors would like to acknowledge the support from Universidad de Monterrey. We express our gratitude to Julio A. Rivera Haro (CIMAV, Monterrey) for ICP-OES measurements and Lilia M. Bautista Carrillo (CIMAV, Monterrey) for DLS measurements.

Conflicts of Interest: The authors declare no conflict of interest.

References

1. Taha-Tijerina, J.; Aviña, K.; Diabb, J.M. Tribological and Thermal Transport Performance of SiO₂-Based Natural Lubricants. *Lubricants* **2019**, *7*, 71. [[CrossRef](#)]
2. Belluco, W.; De Chiffre, L. Surface integrity and part accuracy in reaming and tapping stainless steel with new vegetable based cutting oils. *Tribol. Int.* **2002**, *35*, 865–870. [[CrossRef](#)]
3. Das, A.; Patel, S.K.; Das, S.R. Performance comparison of vegetable oil based nanofluids towards machinability improvement in hard turning of HSLA steel using minimum quantity lubrication. *Mech. Ind.* **2019**, *20*, 506. [[CrossRef](#)]
4. Zubir, B.; Abdul, M.Z.; Abd, A.F.; Said, M.S. The effect of cutting fluid condition on surface roughness in turning of alloy steel. In *Advanced Engineering for Processes and Technologies*; Ismail, A., Abu Bakar, M., Öchsner, A., Eds.; Springer: Cham, Switzerland, 2019; pp. 297–305.
5. Taha-Tijerina, J.J. Thermal transport and Challenges on Nanofluids Performance. In *Microfluidics and Nanofluidics*; Kandelousi, M.S., Ed.; InTech: Rijeka, Croatia, 2018; pp. 215–256.
6. Altavilla, C.; Sarno, M.; Ciambelli, P.; Senatore, A.; Petrone, V. New “chimie douce” approach to the synthesis of hybrid nanosheets of MoS₂ on CNT and their anti-friction and anti-wear properties. *Nanotechnology* **2013**, *24*, 125601. [[CrossRef](#)]
7. Shashidhara, Y.M.; Jayaram, S.R. Vegetable oils as a potential cutting fluid—An evolution. *Tribol. Int.* **2010**, *43*, 1073–1081. [[CrossRef](#)]
8. Koh, M.Y.; Ghazi, T.I.M.; Idris, A. Synthesis of palm based biolubricant in an oscillatory flow reactor (OFR). *Ind. Crops Prod.* **2014**, *52*, 567–574. [[CrossRef](#)]
9. Heikal, E.K.; Elmelawy, M.S.; Khalil, S.A.; Elbasuny, N.M. Manufacturing of environment friendly biolubricants from vegetable oils. *Egypt. J. Pet.* **2017**, *26*, 53–59. [[CrossRef](#)]
10. Krolczyk, G.M.; Maruda, R.W.; Krolczyk, J.B.; Wojciechowski, S.; Mia, M.; Nieslony, P.; Budzik, G. Ecological trends in machining as a key factor in sustainable production—A review. *Clean. Prod.* **2019**, *218*, 601–615. [[CrossRef](#)]
11. Xavier, M.A.; Adithan, M. Determining the influence of cutting fluids on tool wear and surface roughness during turning of AISI 304 austenitic stainless steel. *J. Mater. Process. Technol.* **2009**, *209*, 900–909. [[CrossRef](#)]
12. Benedicto, E.; Carou, D.; Rubio, E.M. Technical, Economic and Environmental Review of the Lubrication/Cooling Systems used in Machining Processes. *Procedia Eng.* **2017**, *184*, 99–116. [[CrossRef](#)]
13. Peña-Parás, L.; Maldonado-Cortés, D.; Taha-Tijerina, J. Eco-Friendly Nanoparticle Additives for Lubricants and Their Tribological Characterization. In *Handbook of Ecomaterials*; Torres Martínez, L.M., Kharissova, O.V., Kharisov, B.I., Eds.; Springer International Publishing: Cham, Switzerland, 2018; pp. 1–21.

14. Taha-Tijerina, J.; Narayanan, T.N.; Avali, S.; Ajayan, P.M. 2D Structures-based Energy Management Nanofluids. In Proceedings of the ASME 2012 International Mechanical Engineering Congress & Exposition IMECE, Houston, TX, USA, 9–15 November 2012. IMECE 2012-87890.
15. Nagendramma, P.; Kumar, P. Eco-Friendly Multipurpose Lubricating Greases from Vegetable Residual Oils. *Lubricants* **2015**, *3*, 628–636. [[CrossRef](#)]
16. Karmakar, G.; Ghosh, P.; Sharma, B. Chemically Modifying Vegetable Oils to Prepare Green Lubricants. *Lubricants* **2017**, *5*, 44. [[CrossRef](#)]
17. Liu, Z.; Sharma, B.K.; Erhan, S.Z.; Biswas, A.; Wang, R.; Schuman, T.P. Oxidation and low temperature stability of polymerized soybean oil-based lubricants. *Thermochim. Acta* **2015**, *601*, 9–16. [[CrossRef](#)]
18. Quinchia, L.A.; Delgado, M.A.; Franco, J.M.; Spikes, H.A.; Gallegos, C. Low-temperature flow behaviour of vegetable oil-based lubricants. *Ind. Crops Prod.* **2012**, *37*, 383–388. [[CrossRef](#)]
19. Erhan, S.Z.; Sharma, B.K.; Perez, J.M. Oxidation and low temperature stability of vegetable oil-based lubricants. *Ind. Crops Prod.* **2006**, *24*, 292–299. [[CrossRef](#)]
20. Reeves, C.J.; Siddaiah, A.; Menezes, P.L. A Review on the Science and Technology of Natural and Synthetic Biolubricants. *J. Bio-Tribo-Corrosion* **2017**, *3*, 11. [[CrossRef](#)]
21. Somashekaraiah, R.; Gnanadhas, D.P.; Kailas, S.V.; Chakravorty, D. Eco-Friendly, Non-Toxic Cutting Fluid for Sustainable Manufacturing and Machining Processes. *Tribol. Online* **2016**, *11*, 556–567. [[CrossRef](#)]
22. Kumar, N. Oxidative stability of biodiesel: Causes, effects and prevention. *Fuel* **2017**, *190*, 328–350. [[CrossRef](#)]
23. Fox, N.J.; Stachowiak, G.W. Vegetable oil-based lubricants-A review of oxidation. *Tribol. Int.* **2007**, *40*, 1035–1046. [[CrossRef](#)]
24. Syahrullail, S.; Kamitani, S.; Shakirin, A. Performance of vegetable oil as lubricant in extreme pressure condition. *Procedia Eng.* **2013**, *68*, 172–177. [[CrossRef](#)]
25. Tripathi, A.; Vinu, R. Characterization of Thermal Stability of Synthetic and Semi-Synthetic Engine Oils. *Lubricants* **2015**, *3*, 54–79. [[CrossRef](#)]
26. Zainal, N.A.; Zulkifli, N.W.M.; Gulzar, M.; Masjuki, H.H. A review on the chemistry, production, and technological potential of bio-based lubricants. *Renew. Sustain. Energy Rev.* **2018**, *82*, 80–102. [[CrossRef](#)]
27. Debnath, S.; Reddy, M.M.; Yi, Q.S. Environmental friendly cutting fluids and cooling techniques in machining: A review. *J. Clean. Prod.* **2014**, *83*, 33–47. [[CrossRef](#)]
28. Sarno, M.; Senatore, A.; Spina, D.; Mustafa, W.A.A. A Tribochemical Boost for Cu Based Lubricant Nano-Additive. *Key Eng. Mater.* **2019**, *813*, 292–297. [[CrossRef](#)]
29. Kumar, K.; Ravi, M. Past and Current Status of Eco-Friendly Vegetable Oil Based Metal Cutting Fluids. *Mater. Today Proc.* **2017**, *4*, 3786–3795. [[CrossRef](#)]
30. Rapeti, P.; Pasam, V.K.; Rao, K.M.; Revuru, R.S. Performance evaluation of vegetable oil based nano cutting fluids in machining using grey relational analysis-A step towards sustainable manufacturing. *J. Clean. Prod.* **2018**, *172*, 2862–2875. [[CrossRef](#)]
31. Wagner, H.; Luther, R.; Mang, T. Lubricant base fluids based on renewable raw materials: Their catalytic manufacture and modification. *Appl. Catal. A Gen.* **2001**, *221*, 429–442. [[CrossRef](#)]
32. Abdalla, H.S.; Patel, S. The performance and oxidation stability of sustainable metalworking fluid derived from vegetable extracts. *Proc. Inst. Mech Eng. Part. B J. Eng. Manuf.* **2006**, *220*, 2027–2040. [[CrossRef](#)]
33. Mannekote, J.K.; Kailas, S.V. The Effect of Oxidation on the Tribological Performance of Few Vegetable Oils. *J. Mater. Res. Technol.* **2012**, *1*, 91–95. [[CrossRef](#)]
34. Barcikowski, S.; Amendola, V.; Marzun, G.; Rehbock, C.; Reichenberger, S.; Zhang, D.; Gökce, B. *Handbook of Laser Synthesis of Colloids*; Universität Duisburg-Essen: Duisburg, Germany, 2016; 150p.
35. Yang, G. *Laser Ablation in Liquids: Principles and Applications in the Preparation of Nanomaterials*; Pan Stanford Publishing: Singapore, 2012.
36. Zhang, D.; Gökce, B.; Barcikowski, S. Laser Synthesis and Processing of Colloids: Fundamentals and Applications. *Chem. Rev.* **2017**, *117*, 3990–4103. [[CrossRef](#)]
37. Zhang, D.; Liu, J.; Li, P.; Tian, Z.; Liang, C. Recent Advances in Surfactant-Free, Surface-Charged, and Defect-Rich Catalysts Developed by Laser Ablation and Processing in Liquids. *ChemNanoMat* **2017**, *3*, 512–533. [[CrossRef](#)]
38. Johnny, J.; Sepulveda, G.S.; Krishnan, B.; Avellaneda, D.; Shaji, S. Nanostructured SnS₂ Thin Films from Laser Ablated Nanocolloids: Structure, Morphology, Optoelectronic and Electrochemical Properties. *ChemPhysChem* **2018**, *19*, 2902–2914. [[CrossRef](#)] [[PubMed](#)]

39. Kozuka, H.; Yamano, A.; Fujita, M.; Uchiyama, H. Aqueous dip-coating route to dense and porous silica thin films using silica nanocolloids with an aid of polyvinylpyrrolidone. *J. Sol-Gel Sci. Technol.* **2012**, *61*, 381–389. [[CrossRef](#)]
40. Zuñiga-Ibarra, V.A.; Shaji, S.; Krishnan, B.; Johnny, J.; Sharma, K.S.; Avellaneda, D.A.; Martinez, J.A.A.; Roy, T.K.D.; Ramos-Delgado, N.A. Synthesis and characterization of black TiO₂ nanoparticles by pulsed laser irradiation in liquid. *Appl. Surf. Sci.* **2019**, *483*, 156–164. [[CrossRef](#)]
41. Shaji, S.; Vinayakumar, V.; Krishnan, B.; Johnny, J.; Sharma, K.S.; Flores, J.M.; Sepulveda, S.; Avellaneda, D.A.; Castillo, G.A.; Aguilar, J.A. Copper antimony sulfide nanoparticles by pulsed laser ablation in liquid and their thin film for photovoltaic application. *Appl. Surf. Sci.* **2019**, *476*, 94–106. [[CrossRef](#)]
42. Rodriguez-Vela, D.L.; Krishnan, B.; Aguilar-Martinez, J.A.; Loredano, S.L.; Shaji, S. AgSb(S_xSe_{1-x})₂ thin films by rapid thermal processing of Sb₂S₃-Ag-Se thin films for photovoltaic applications. *Phys. Status Solidi* **2016**, *13*, 47–52.
43. Ganguly, S.; Das, P.; Bose, M.; Das, T.K.; Mondal, S.; Das, A.K.; Das, N.C. Sonochemical green reduction to prepare Ag nanoparticles decorated graphene sheets for catalytic performance and antibacterial application. *Ultrason. Sonochem.* **2017**, *39*, 577–588. [[CrossRef](#)]
44. Lokhande, A.C.; Babar, P.T.; Karade, V.C.; Jang, J.S.; Lokhande, V.C.; Lee, D.J.; Kim, I.C.; Patole, S.P.; Qattan, I.A.; Lokhande, C.D.; et al. A viable green route to produce Ag nanoparticles for antibacterial and electrochemical supercapacitor applications. *Mater. Today Chem.* **2019**, *14*, 100181. [[CrossRef](#)]
45. Szczerek, M.; Tuszyński, W. A method for testing lubricants under conditions of scuffing. Part, I. Presentation of the method. *Tribotest* **2002**, *8*, 273–284. [[CrossRef](#)]
46. Peña-Parás, L.; Taha-Tijerina, J.; García, A.; Maldonado, D.; Nájera, A.; Cantú, P.; Ortiz, D. Thermal transport and tribological properties of nanogreases for metal-mechanic applications. *Wear* **2015**, *332–333*, 1322–1326. [[CrossRef](#)]
47. Taha-Tijerina, J.; Peña-Paras, L.; Narayanan, T.N.; Garza, L.; Lapray, C.; Gonzalez, J.; Palacios, E.; Molina, D.; García, A.; Maldonado, D.; et al. Multifunctional nanofluids with 2D nanosheets for thermal and tribological management. *Wear* **2013**, *302*, 1241–1248. [[CrossRef](#)]
48. Peña-Parás, L.; Taha-Tijerina, J.; García, A.; Maldonado, D.; González, J.A.; Molina, D.; Palacios, E.; Cantú, P. Antiwear and Extreme Pressure Properties of Nanofluids for Industrial Applications. *Tribol. Trans.* **2014**, *57*, 1072–1076. [[CrossRef](#)]
49. Taha-Tijerina, J.; Castañón-Guitrón, B.; Peña-Parás, L.; Tovar-Padilla, M.; Alvarez-Quintana, J.; Maldonado-Cortés, D. Impact of silicate contaminants on tribological and thermal transport performance of greases. *Wear* **2019**, *426–427*, 862–867. [[CrossRef](#)]
50. Kanakillam, S.S.; Shaji, S.; Krishnan, B.; Vazquez-Rodriguez, S.; Martinez, J.A.A.; Palma, M.I.M.; Avellaneda, D.A. Nanoflakes of zinc oxide: cobalt oxide composites by pulsed laser fragmentation for visible light photocatalysis. *Appl. Surf. Sci.* **2020**, *501*, 144223. [[CrossRef](#)]
51. LotfizadehDehkordi, B.; Kazi, S.N.; Hamdi, M.; Ghadimi, A.; Sadeghinezhad, E.; Metselaar, H.S.C. Investigation of viscosity and thermal conductivity of alumina nanofluids with addition of SDBS. *Heat Mass Transf.* **2013**, *49*, 1109–1115. [[CrossRef](#)]
52. Taha-Tijerina, J.J.; Narayanan, T.N.; Tiwary, C.S.; Lozano, K.; Chipara, M.; Ajayan, P.M. Nanodiamond-based thermal fluids. *ACS Appl. Mater. Interfaces* **2014**, *6*, 4778–4785. [[CrossRef](#)] [[PubMed](#)]
53. Taha-Tijerina, J.; Narayanan, T.N.; Gao, G.; Rohde, M.; Tsentelovich, D.A.; Pasquali, M.; Ajayan, P.M. Electrically insulating thermal nano-oils using 2D fillers. *ACS Nano* **2012**, *6*, 1214–1220. [[CrossRef](#)]
54. Jang, S.P.; Choi, S.U.S. Role of Brownian motion in the enhanced thermal conductivity of nanofluids. *Appl. Phys. Lett.* **2004**, *84*, 4316. [[CrossRef](#)]
55. Azmi, W.H.; Sharma, K.V.; Mamat, R.; Najafi, G.; Mohamad, M.S. The enhancement of effective thermal conductivity and effective dynamic viscosity of nanofluids—A review. *Renew. Sust. Energ. Rev.* **2016**, *53*, 1046–1058. [[CrossRef](#)]

56. Dai, W.; Kheireddin, B.; Gao, H.; Liang, H. Roles of nanoparticles in oil lubrication. *Tribol. Int.* **2016**, *102*, 88–98. [[CrossRef](#)]
57. Chen, Y.; Renner, P.; Liang, H. Dispersion of Nanoparticles in Lubricating Oil: A Critical Review. *Lubricants* **2019**, *7*, 7. [[CrossRef](#)]



© 2020 by the authors. Licensee MDPI, Basel, Switzerland. This article is an open access article distributed under the terms and conditions of the Creative Commons Attribution (CC BY) license (<http://creativecommons.org/licenses/by/4.0/>).